

Formation of fused aggregates under long-term microgravity conditions aboard the ISS with implications for early Solar System particle aggregation

T. E. Koch^{1*}, D. Spahr¹, B. J. Tkalcec¹, O. Christ², P.-T. Genzel¹, M. Lindner¹, D. Merges¹, F. Wilde³, B. Winkler¹, F. E. Brenker^{1,4}

¹Institute of Geosciences, Goethe University Frankfurt, Altenhoferallee 1, 60438 Frankfurt am Main, Germany ²Department of Geoscience, University of Padua, Via Gradenigo 6, 35131 Padua, Italy ³Helmholtz-Zentrum Hereon, Max-Planck Strasse 1, 21502 Geesthacht, Germany ⁴Hawai'i Institute of Geophysics and Planetology, School of Ocean and Earth Science and Technology, University of Hawai'i at Mānoa, 1680 East-West Road, Honolulu, HI 96822, USA
*t.koch@em.uni-frankfurt.de



INTRODUCTION

The aggregation of particles in the Solar Nebula is generally considered as the first process leading to planet formation [1,2]. Refractory inclusions, such as calcium-aluminum-rich inclusions (CAIs) are likely witnesses of early aggregation processes. The chemical properties of CAIs and AOA have been intensively studied [e.g. 3]. Their structural characteristics, such as morphologies, texture and porosity bear further knowledge about the processes regarding the circumstances of aggregation, reheating, annealing, recrystallization, compaction as well as Solar Nebula dynamics and material transportation (4-6). In the study presented here, we show the formation of aggregates using flash-heating under microgravity conditions which can be linked to the formation of refractory inclusions with regard to their morphology and microstructure.

EXPERIMENTAL

Mg₂SiO₄ dust particles (Fig. 1) were exposed to arc discharges inside a glass sample chamber aboard the ISS. The experiments were filmed (Fig. 2). In total, 81 arc discharges with energies of 5–8 J were induced, see [7].

The sample material was analyzed after sample return to Earth using SEM and synchrotron micro-CT [8].

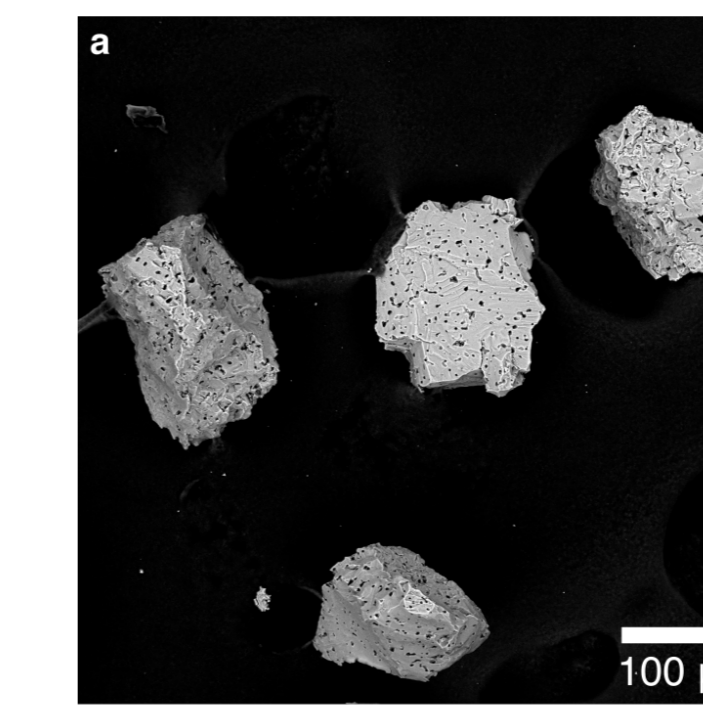


Fig. 2. Focus-stacked SEM BSE images of representative initial particles.

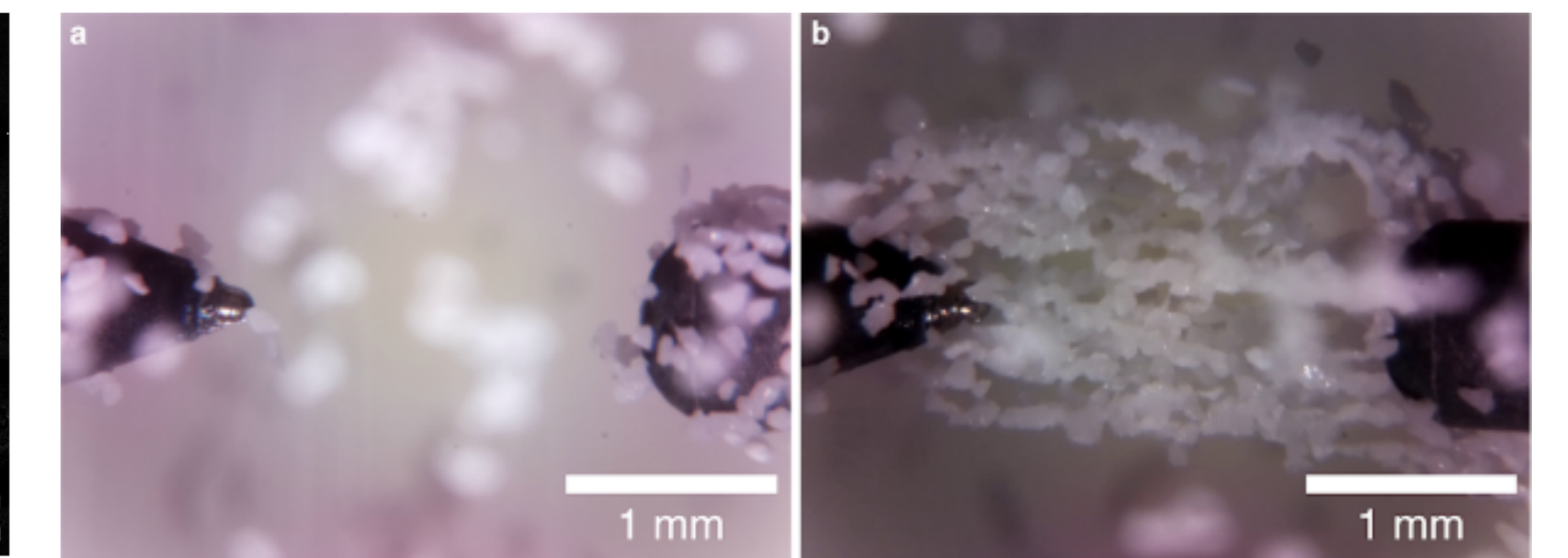


Fig. 2. (a) The field of view prior to the arc discharge experiments. The tips of the electrodes are shown on opposite sides of the image. (b) The particles formed chains along the field lines between the two electrodes prior to the third arc discharge.

RESULTS

- more than 100 transformed samples could be detected after sample return
- samples were studied with scanning electron microscopy and synchrotron micro-CT

- different types of aggregates were formed:

- boomerang-shaped, bend aggregates (Fig. 3a)
- elongated aggregates (Fig. 3d,e)
- one aggregate with a flat disk (Fig. 3c,d)
- aggregates with a massy center (Fig. 5)

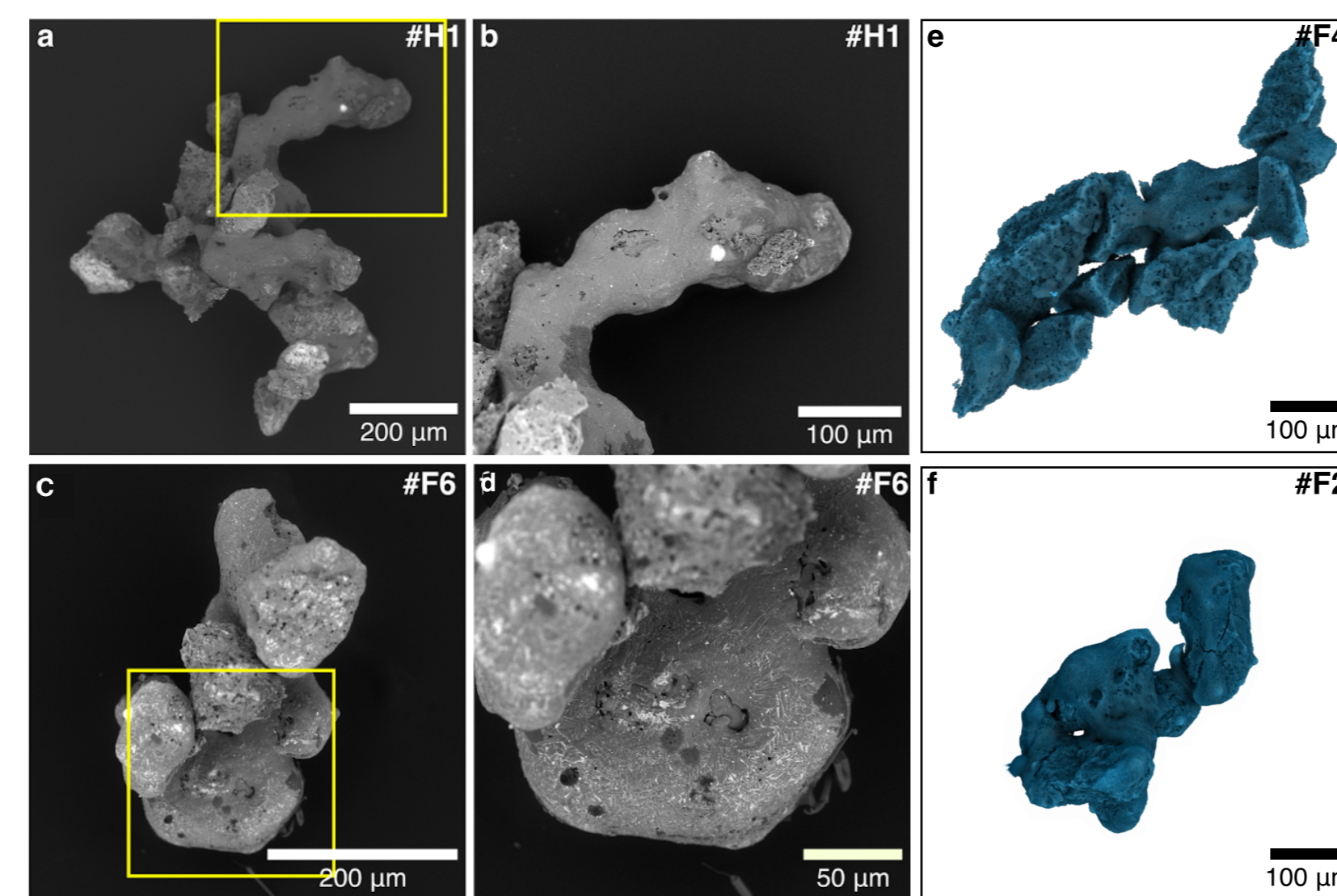


Fig. 3. Focus-stacked SEM BSE images (a-d) and CT projections (e-f) of formed aggregates (a) A boomerang-shaped aggregate (b) Close-up of the aggregate in a. (c) An aggregate with a flat disk. (d) Close-up of the disk. The precipitations which appear white in the BSE images consist of tungsten, which was sputtered from the electrodes. (e,f) Representative elongated aggregates.

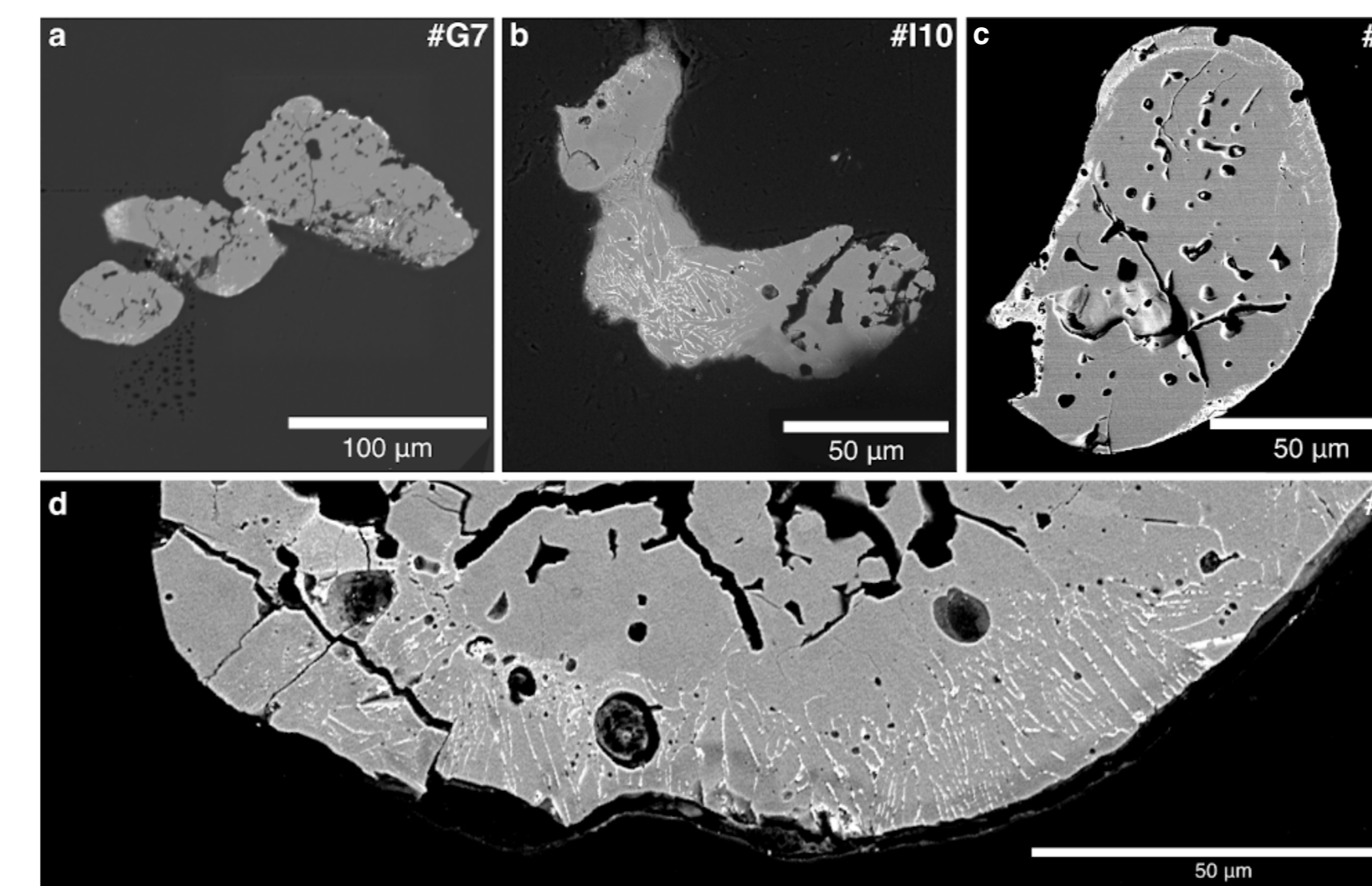


Fig. 4. SEM BSE images of polished aggregates. All precipitations which appear white in the images are tungsten. Grains which are fused show different degrees of melting (a,b). Some grains are surrounded by igneous rims (c,d).

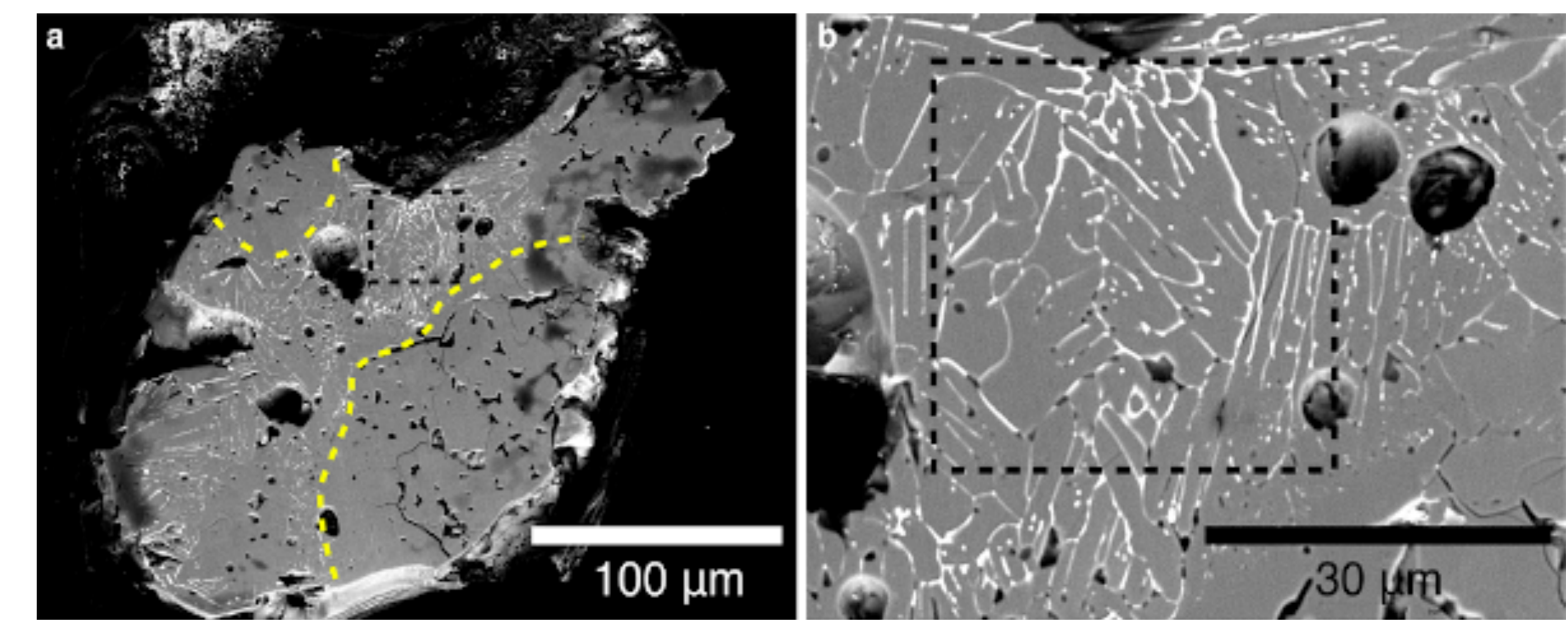


Fig. 5. SEM BSE images of a polished aggregate with a massy center. (a) Cross section of the aggregate. The yellow lines show the boundaries between areas with the initial microstructure and areas which were molten. (b) Close-up of the molten area. The individual grains which formed the aggregate cannot be distinguished anymore. The aggregate has probably formed from the collision of different initial grains, where some grains were completely molten.

AGGREGATION & COOLING

The particle velocities after arc discharges were analyzed and the velocities were used to determine the mean time between two collisions (Fig. 7c) [9]. Aggregates which consist of 20 particles must have formed within > 0.5 s. The temperature of particles after arc discharges were also determined (Fig. 7b) [10]. Particles probably stick in collisions at $T > 1400$ K. Consequently, aggregates were formed in < 0.5 s.

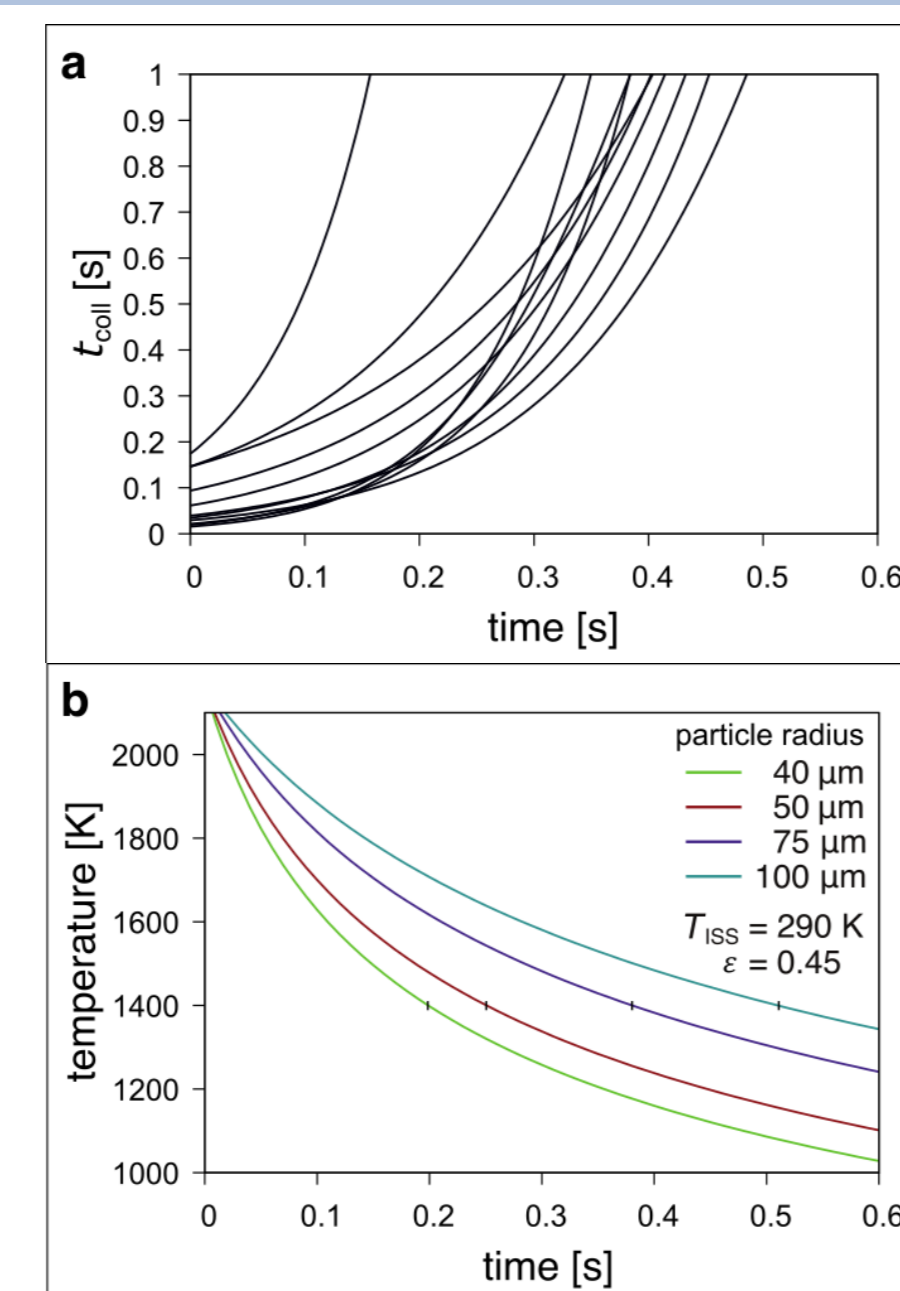


Fig. 6. Collision times t_{coll} of particles inside the sample chamber and cooling rates of the particles after arc discharges. (a) t_{coll} versus the time after the arc discharges is plotted for several grains after different arc discharges. (b) Calculated temperatures of particles with different radii versus time after the arc discharges inside the sample chamber.

COMPARISON TO NATURAL CAIs

The morphologies of the aggregates formed in the experiment were compared with natural CAIs. A random sample of representative CAIs in the CV3 chondrite NWA 13656 was analyzed. All characteristic morphologies of the formed aggregates could be found in natural refractory inclusions (Fig. 7).

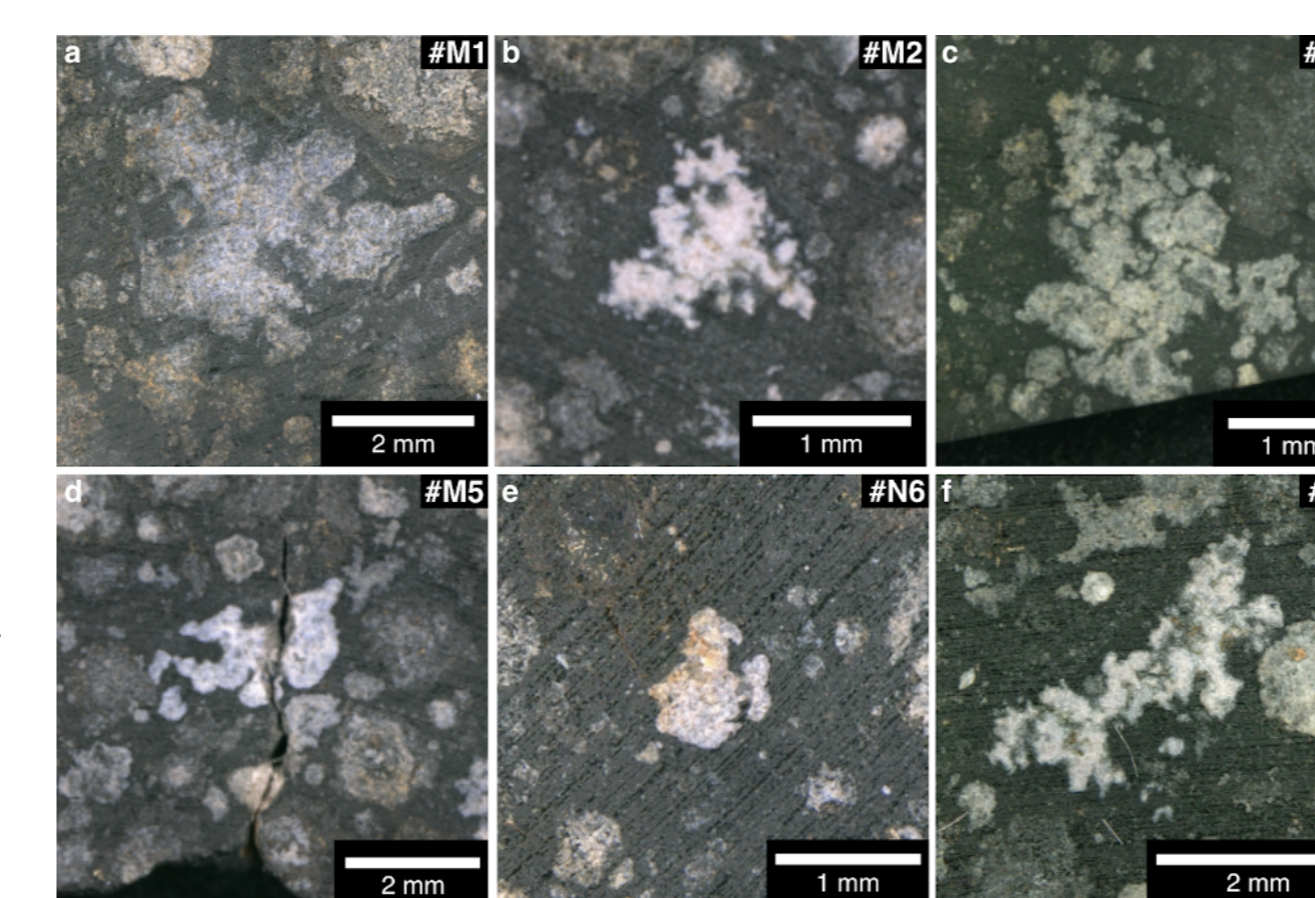


Fig. 7. Photographs of irregular inclusions on slices of NWA 13656. (a) Inclusion with four wings. (b) Tringle-shaped inclusion (c) Three-winged inclusion. (d) Inclusion with a massy center and two attached nodular wings. (e) Inclusion with a massy center and several attached nodules. (f) Elongated inclusion.

CONCLUSION

The experimentally produced fused aggregates resemble many specific morphological CAI characteristics reported in the literature, such as the fluffy-type CAI morphologies, igneous CAI textures with relict grains, disk-like CAIs and Wark-Lovering rims. The fractal structures formed in the experiment are very stable which could explain why the fractal structures of fluffy-type CAIs survived transportation to the chondrite accretion region and chondrite parent body formation. The high acceleration of particles would lead to disk and bowl-shaped CAIs. Collisions of CAI nodules with different degrees of melting can form igneous and compound CAIs. In summary, these results imply, that periodically repeated local (flash-)heating events with subsequent aggregation of particles could have been involved in CAI formation after their condensation.

ACKNOWLEDGMENTS



REFERENCES

- [1] Blum & Wurm 2008 [2] Dominik et al. 2006 [3] Krot et al. 2019 [4] Komatsu et al. 2001 [5] Rubin 2012 [6] Lorenz et al. 2019 [7] Spahr et al. 2020 [8] Wilde et al. 2016 [9] Nakagawa et al. 1981 [10] Ciesla et al. 2004